Phenomenological law for the acoustic reflection by an array of cylindrical cavities in a soft elastic medium

M Thieury, Valentin Leroy, J Dassé, A Tourin

Phenomenological law for the acoustic reflection by an array of cylindrical cavities in a soft elastic medium

M. Thieury,[1] V. Leroy,[2] J. Dassé,[3] and A. Tourin[4, a)]
[1)] *Institut Langevin, ESPCI Paris, PSL University, CNRS, Paris, France*
[2)] *Laboratoire Matière et Systèmes Complexes, Université de Paris, CNRS, Paris, France*
[3)] *Thales Underwater Systems,Valbonne, France*
[4)] *Institut Langevin, ESPCI Paris, PSL University, CNRS, 75238 Paris, France*

(Dated: 1 October 2020)

We propose a phenomenological model, built from results obtained by finite element numerical simulations, for the transmission and reflection of acoustic waves by a two-dimensional array of cylindrical cavities in a soft elastic medium. We show that the acoustic properties of a cylindrical cavity can be described by two geometrical parameters: its aspect ratio (AR), and the radius of the sphere of equivalent volume. Cylinders with AR close to one are acoustically similar to spheres, whereas flat cylinders exhibit a lower resonance frequency and an increased damping, due to their ability to emit shear waves. We provide an example of how our new phenomenological analytical model can help to design thin coatings that can turn strong acoustic reflectors into good absorbers.

I. INTRODUCTION

Soft elastic media exhibit interesting acoustic properties when they are perforated. It comes from the strong monopolar acoustic response of a cavity when it is embedded in a medium that easily deforms. There is an extensive literature on the acoustic transmission through perforated panels,[1–8] mainly focused on the ability of these structures to absorb acoustic energy on a thickness shorter than the wavelength. The shape of the cavities is an important issue. On the one hand, simple shapes, such as spheres or infinite cylinders, offer the advantage of being theoretically simpler to model, leading to analytical expressions for the transmission and reflection by an array of cavities.[9,10] On the other hand, other shapes, such as cylinders or disks, lead to more tedious calculations but are closer to real applications, and sometimes exhibit better performance. As an intermediate case, let us cite the ellipsoid, which allows to investigate the case of elongated shapes with analytical calculations.[11–13] Elongated cavities are of particular interest because, for a given volume, they can be thinner and thus be embedded in thinner structures. Recently, Calvo *et al.*[14] showed experimentally that flat cylindrical cavities were a promising option for reaching low frequency absorption with a thin layer of elastomer. Sharma *et al.*[15] derived a model that is suitable for these experiments, considering the flat cylinders as two-dimensional disks. In this article, we explore the transition between spherical cavities and cylinders of increasing aspect ratio (AR), from AR= 1 for "sphere-like" cylinders, to AR= 24 for "pancake-like" ones.

Our aim is to derive an analytical model that is effective for both spherical and cylindrical cavities. Such a model could be a useful tool for the optimization of acoustic super-absorbers, as guideline to initiate numerical simulations. Finite-element methods (FEM) remain of course the most powerful way to evaluate the performance of a perforated panel, in particular because they allow to explore exotic shapes for the cavities. Their main drawback is to be time-consuming, which limits the number of configurations one can explore in an optimization process. Note, however, that a recent trend of using axisymmetric unit cell for FEM has proven to lead to very efficient calculations[16], opening the way for new designs with wine glass-shaped cavities for example.[8] Nevertheless, despite all the merits of FEM, an analytical model is always useful, as it can be used as a quick first guess to initiate a systematic numerical optimization, and also because it often provides a physical insight on the mechanism responsible for the better performance of a given configuration.

In this article, we follow a phenomenological approach to investigate the problem of the shape of cavities. In section II, we start by the ideal case of spherical cavities, and illustrate how having an analytical model is useful for optimization purposes, *i.e.* for selecting the best cavities radius and concentration in order to maximize the acoustic absorption at a given frequency. Section III is devoted to numerical simulations with a single cavity. The idea is to determine how a cylindrical cavity scatters a longitudinal wave, depending on its aspect ratio. We show that this scattering behavior shares similarities with the one of a sphere, and we propose a phenomenological scattering function, which depends on the volume and aspect ratio of the cavity. An important result is the evidence of a new source of damping that does not exist for spheres: flat cylinders are showed to convert part of the incoming longitudinal wave energy into shear waves. The next step, in section IV, is to use the established phenomenological function for calculating the response of an array of cavities. We show that our phenomenological model gives reasonable predictions when compared to numerical simulations and experiments. We finally discuss how the new source of damping for cylinders can be exploited to design thinner acoustic absorbers, while widening their frequency bandwidth.

II. ANALYTICAL MODEL FOR AN ARRAY OF SPHERICAL CAVITIES

Let us consider an array of identical spherical voids in an elastomer, as depicted in figure 1a. We note a the radius of

[a)] Electronic mail: arnaud.tourin@espci.fr

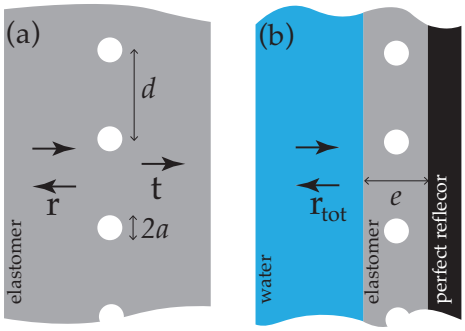

FIG. 1. Schematics of the two configurations considered. (a) The metascreen: a single array of spherical cavities in an elastomer. (b) A metascreen of thickness e placed, in water, on a perfect reflector.

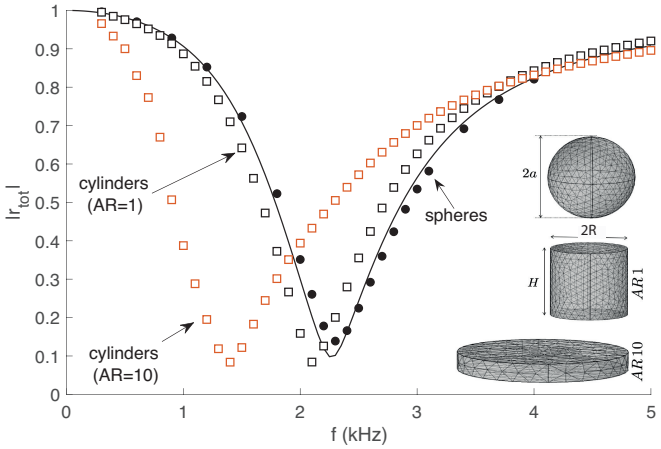

FIG. 2. Amplitude of reflection $r_{\rm tot}$ for a metascreen on a perfect reflector. For spherical cavities of radius $a = 4.5\,$mm with a spacing $d = 125\,$mm, the reflection is minimal at 2.15 kHz, as predicted by the model (solid line) and confirmed by the numerical simulations (black dots). For cylindrical cavities of same volume but different aspect ratios (AR), the reflection is slightly modified for AR=1 (black squares), and significantly shifted to lower frequencies for AR=10 (red squares).

the holes, and d the distance between two neighbors. When a plane wave $p\exp[\mathrm{i}(kx-\omega t)]$ impinges on this metascreen at normal incidence, part of its energy is reflected back, part is absorbed, and another part is transmitted. It was shown that, provided that the array is not too concentrated ($d/a > 5$), the transmission and reflection coefficients could be evaluated by the following analytical expressions:[9]

$$t = 1 + r, \tag{1}$$

$$r = \frac{\mathrm{i}Ka}{\left(\frac{\omega_0}{\omega}\right)^2 - I - \mathrm{i}(\delta + Ka)}, \tag{2}$$

with

$$K = \frac{2\pi}{kd^2}, \tag{3a}$$

$$\omega_0 = \sqrt{\frac{4G}{\rho a^2}}, \tag{3b}$$

$$I = 1 - Ka\sin\left(\frac{kd}{\sqrt{\pi}}\right) \simeq 1 - 2\sqrt{\pi}\frac{a}{d} \quad \text{for } kd \ll 1 \tag{3c}$$

$$\delta = 4\eta/(\rho a^2 \omega), \tag{3d}$$

where k is the wavenumber of longitudinal waves in the elastomer, ρ the density of the elastomer, and G, η its shear modulus and viscosity. Equations (1) and (2) predict that r and t are frequency dependent, with a maximum of reflection (and minimum of transmission) for $\omega = \omega_0/\sqrt{I}$, *i.e.* close to the resonance of a single cavity. The width of this peak of reflection is controlled by two damping terms: δ for visous losses, and Ka for super-radiation. At its maximum of amplitude, the reflection coefficient is given by the simple formula

$$r = -\frac{Ka}{\delta + Ka}. \tag{4}$$

As expected for a soft baffle, the reflection coefficient is negative. Interestingly, its value depends on the distance d between the cavities. Indeed, the reflection can take any values between 0, when Ka is low (large d), and -1, when Ka is large (small d). This dependence can be used to optimize the energy absorption of the metascreen.[17] The case depicted in Fig. 1b is of particular interest: a metacreen of thickness e placed, in water, on the surface of a perfect rigid reflector. If the elastomer is impedance-matched with water, the multiple reflection paths are easy to compute and lead to a total reflection given by

$$r_{\rm tot} = r + \frac{t^2\exp(\mathrm{i}ke)}{1 - r\exp(\mathrm{i}ke)} \tag{5a}$$

$$\simeq \frac{1+3r}{1-r} \quad \text{for } ke \ll 1. \tag{5b}$$

Equation (5b) tells us that the perfect reflector can be turned into a perfect absorber if the layer of cavities is designed in such a way that its reflection coefficient is $r = -1/3$. According to Eq. (4), this can be achieved if $\delta = 2Ka$, *i.e.* for $d^2 = \pi\rho a^3 v/\eta$, where v is the speed of sound in the elastomer.

As an example of optimization, let us imagine that we want to minimize the reflection at 2.15 kHz with an elastomer whose shear modulus is $G = 1\,$MPa, viscosity $\eta = 33\,$Pa.s, speed of sound $v = 1350\,$m/s, and density $\rho = 1100\,$kg/m^3. We first need to choose the radius of the holes to adapt their resonance frequency. Following Eq. (3b), it leads to $a = 4.5\,$mm. Then, the distance between the holes must be chosen to satisfy the $\delta = 2Ka$ criterion, which gives $d = 125\,$mm. Fig. 2 compares analytical expression (5b) to a numerical simulation (black dots in the figure), with $e = 35\,$mm. As predicted, there is a minimum of reflection at 2.15 kHz, which corresponds to an acoustic wavelength 20 times larger than the thickness of the coating. This result illustrates the interest of having an analytical expression for the acoustic response of the metascreen: knowing the physical parameters of the elastomer at hand, it is easy to determine the best geometrical parameters to optimize the performance at a given frequency.

However, when the holes are not spherical (which is often the case in practical applications), the analytical solution

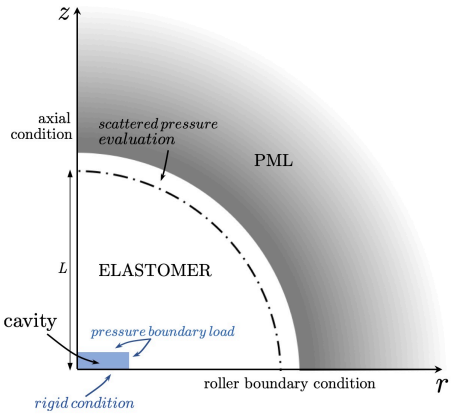

FIG. 3. Schematic (not to scale) of the computational domain for determining the scattering function of a cavity. The displacement field is axisymmetric about the z axis and antisymmetric about $z = 0$. A perfectly matched layer (PML) is used to simulate an infinite domain, and the far-field wave emitted by the cavity is measured at distance L.

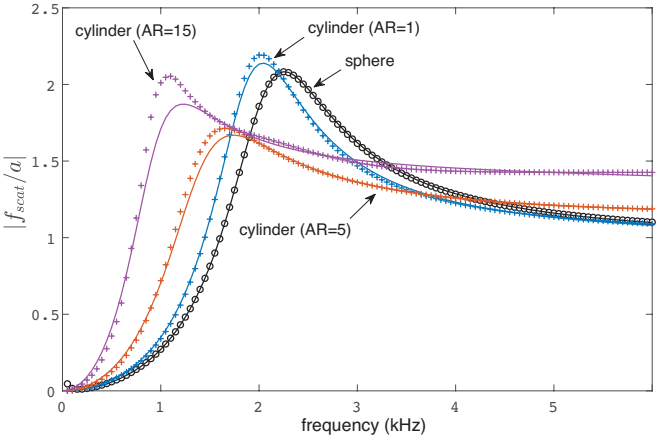

FIG. 4. Amplitude of scattering functions for a sphere (black) and for cylinders with three different aspect ratio: 1 (blue), 5 (red) and 15 (purple). Here the equivalent radius is $a = 4.5$ mm. Symbols show the results from the numerical simulations. Solid lines correspond to Eq. (7) for the sphere (no fitting parameters) and Eq. (8) for the cylinders, with parameters obtained by the fitting procedure described in the text.

is *a priori* not available. Luckily, like for air bubbles in liquids,[18,19] the acoustics of a cavity in an elastomer is mainly governed by its volume[1], provided that the cavity is not too elongated. Hence, if one considers a cylindrical cavity with radius R and height H, all the previous equations can be applied by considering the sphere of equivalent radius:

$$a = (3R^2H/4)^{1/3}. \tag{6}$$

As shown in Fig. 2, this approximation is good as long as the aspect ratio of the cylinder (AR$= 2R/H$) is close to one. For AR$= 1$ (black squares in Fig. 2), the reflection coefficient remains close to the analytical prediction. For flatter cylinders, however, one observes a significant deviation. It means that, unsurprisingly, the aspect ratio of the cylinder plays a role in its acoustic response.

III. SCATTERING BY A CYLINDRICAL CAVITY

To investigate the effect of the aspect ratio, we performed numerical simulations with a single cylinder in a soft elastic medium. We used the same configuration as Calvo *et al.*[14], with a geometry depicted in Fig. 3. A pressure load $p\exp[-\mathrm{i}\omega t]$ is applied on the surface of the cavity and we record the pressure field at distance L. It allows us to determine the scattering function of the cavity, assuming that it radiates a spherical wave $p(f_{\mathrm{scat}}/L)\exp[\mathrm{i}(kL-\omega t)]$.

Figure 4 shows the magnitude of the scattering function obtained for different types of cavities: a sphere of radius $a = 4.5$ mm, and cylinders of the same volume but different aspect ratios. A distance of $L = 140$ mm was taken for evaluating the scattered field. For the sphere, the expected law

$$f_{\mathrm{scat}} = \frac{a}{(\omega_0/\omega)^2 - 1 - \mathrm{i}(\delta + ka)} \tag{7}$$

is recovered, as shown by the black symbols in Fig. 4. For the cylinders, the response deviates from the sphere's one when AR increases. In particular, the frequency of the maximum of scattering decreases when the cylinder is flattened, which is consistent with the behavior already noticed in Fig. 2. One can also notice that the height of the maximum and the width of the resonance are both affected by the aspect ratio. However, even though it changes, the general shape of the scattering function remains that of a lorentzian response function. Hence the idea of looking for a law similar to (7):

$$f_{\mathrm{scat}} = \frac{Aa}{(B\omega_0/\omega)^2 - 1 - \mathrm{i}(C\delta + Dka)}, \tag{8}$$

where a is given by Eq. (6), and A, B, C and D are four non-dimensional parameters accounting for the shape of the cylinder. A characterizes the scattering power of the inclusion, B is related to the shift of the resonance frequency, C is a viscous factor, while D is a scattering factor.

To determine the four parameters, we re-write Eq. (8) in the following form

$$\mathrm{Re}\left[\frac{a}{f_{\mathrm{scat}}}\right] = \frac{(B\omega_0/\omega)^2 - 1}{A}, \tag{9}$$

$$-\mathrm{Im}\left[\frac{a}{f_{\mathrm{scat}}}\right]\frac{\omega}{\omega_1} = \frac{4C}{A} + \frac{D}{A}\frac{\omega^2}{\omega_1\omega_2}, \tag{10}$$

where $\omega_1 = \eta/(\rho a^2)$ and $\omega_2 = v/a$. Thus, a linear fitting of $\mathrm{Re}(a/f_{\mathrm{scat}})$ as a function of $(\omega_0/\omega)^2$ gives us access to A and B. Another linear fitting of $-\mathrm{Im}(a/f_{\mathrm{scat}})\omega/\omega_1$ as a function of $\omega^2/\omega_1\omega_2$ leads to C and D. We show in Fig. 4 how this procedure allows us to use Eq. (8) to capture correctly the numerical results.

By doing linear fittings on data coming from different simulations, we can investigate how parameters A, B, C and D vary with AR. Our hypothesis is that AR is the main parameter to determine the acoustic behavior of a cylinder. To test this hypothesis, we modified the properties of the matrix in the

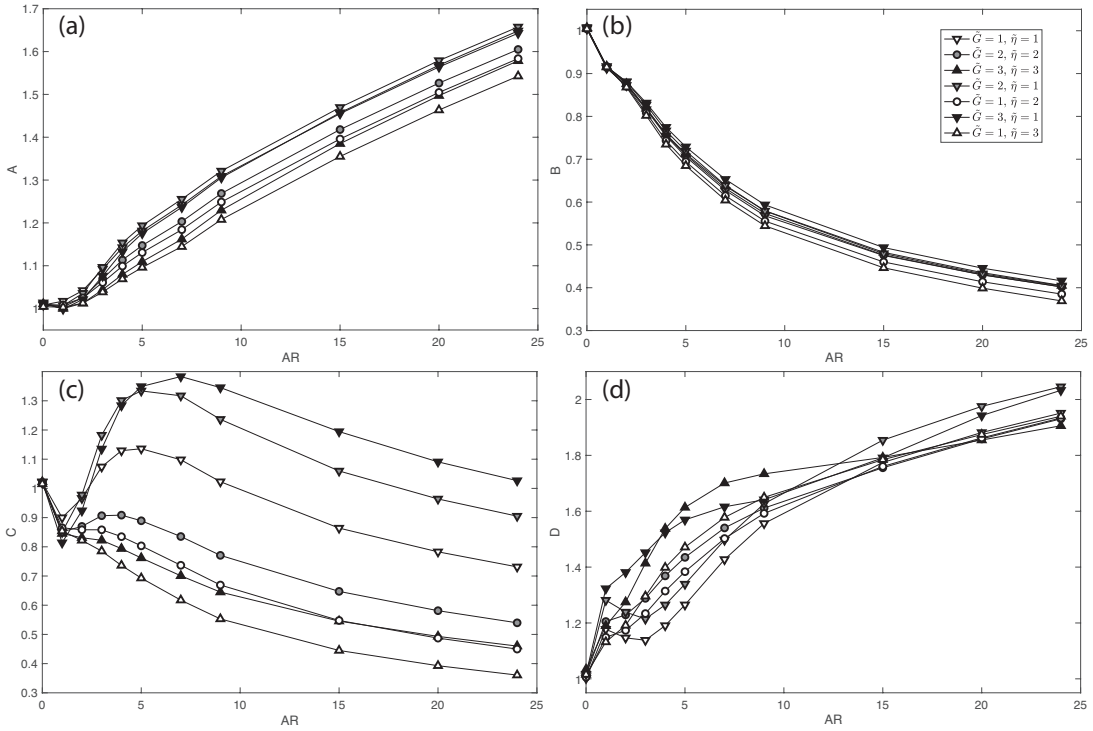

FIG. 5. Parameters A, B, C and D as functions of AR, for simulations with different shear moduli and viscosities. Symbols indicate the viscosity (downside triangles for low η, upside triangles for high η), and their grey level indicates the shear modulus (dark for high G, white for low G). A reasonable collapse of the data for different G and η is obtained for A, B and D. For C, there is clearly a strong influence of G and η. For convenience, results for the spherical cavity are displayed at AR$=0$ (no results are shown for elongated cylinders, with AR<1).

simulation. For example, starting from our reference values of $G = 1\,\text{MPa}$ and $\eta = 33\,\text{Pa.s}$ for the rheology, we applied multiplication factors (noted $\tilde{G}$ and $\tilde{\eta}$ in Fig. 5's legend) of 2 or 3. As shown, in Fig. 5, for A, B and D we obtain reasonable collapses of all the curves plotted as functions of AR for different rheological parameters. It confirms that, within the range of parameters we explored, AR gives a good indication of how a cylinder will be acoustically different from the sphere of same volume. In particular, we find that B is a decreasing function of AR, which is in line with the observed decrease of the resonance frequency when a cylinder is flattened (Fig. 4).

For C, however, the collapse is not satisfactory, which is a sign that another phenomenon is at play in the response of the cylinder. Moreover, one would expect C to be identical to B^2 because, in Eq. (8), the sum of the terms $(B\omega_0/\omega)^2 = 4B^2/(\rho a^2\omega^2)\times G$ and $-\mathrm{i}C\delta = -4\mathrm{i}C/(\rho a^2\omega^2)\times\eta\omega$ must be proportional to the complex shear modulus $G-\mathrm{i}\omega\eta$. It means that $C\delta$ in Eq. (8) should be replaced by $B^2\delta+\omega_3/\omega$, where ω_3 is a new angular frequency. We can evaluate it by subtracting B^2 to C: $\omega_3 = (C-B^2)4\eta/(\rho a^2)$. As shown in Fig 6, it gives a much better collapse of the different curves. The origin of this new damping term, which does not exist when the cavity is spherical, can be identified by looking at the displacement fields obtained in the numerical simulation. Fig. 7 shows examples of the fields for a AR=1 cylinder (left), and for a AR=5 one (right). In both cases, the pressure fields (color) are quite uniform, which is expected given the large wavelength ($\lambda = 84\,\text{cm}$). The displacement fields, on the other hand, are very different. For the AR=5 case, the cavity visibly emits a wave, in the $\pi/4$ direction. The wavelength being of the order of 2 cm, this wave can be identified as a shear wave. Note that this phenomenon was already observed by Calvo *et al.*[14], and that this new source of damping was taken into account for 2D disks by Sharma *et al.*[15]

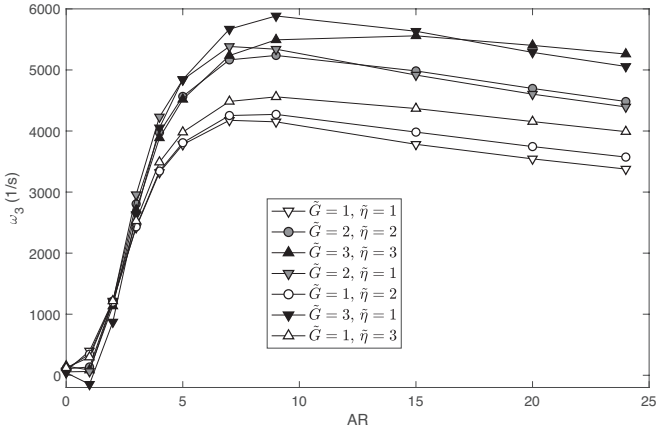

FIG. 6. Instead of parameter C, which does not lead to a good collapse of the data (see Fig. 5), we plot $\omega_3 = (C-B^2)4\eta/(\rho a^2)$ as a function of AR. It leads to a better collapse, with still a noticeable influence of G: the darker the symbols, the higher ω_3 in the large AR limit.

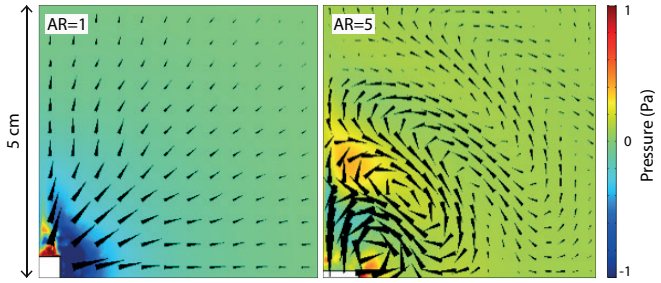

FIG. 7. Pressure (color) and displacement (arrows) fields, at 1.6 kHz, for AR=1 (left) and AR=5 (right) cylinders. On the right, the displacement field displays a 2 cm wavelength, compatible with the emission of a shear wave in the elastomer (shear velocity is $c_s = 30$ m/s for the soft medium used in the simulations).

In Fig. 6 we can notice that there is still an influence of G: for AR>10, ω_3 increases with G. We find that it follows a scaling law close to $\omega_3 \sim G^{1/4}$. Besides, when we change the size of the cavity, we find that $\omega_3 \sim 1/a$. Finally, we propose the following empirical law for the scattering function of a cylindrical cavity:

$$f_{\text{scat}} = \frac{Aa}{\left(B\frac{\omega_0}{\omega}\right)^2 - 1 - \mathrm{i}(B^2\delta + \beta\frac{G^{1/4}}{a\omega} + Dka)}, \qquad (11)$$

with

$$A = 1 + 0.029(\text{AR} - 1), \qquad (12a)$$
$$B = 1/(1 + 0.079\text{AR}), \qquad (12b)$$
$$D = 1 + \sqrt{\text{AR}}/5, \qquad (12c)$$
$$\beta = \frac{\text{AR}^3}{40 + \text{AR}^{3.2}} \quad \text{m.Pa}^{-1/4}/\text{s}. \qquad (12d)$$

Expressions (12) for A, B, D and β were chosen to give the correct trend for the AR-dependence, as shown by the red plots in Fig. 8. This figure proposes a general view of all the numerical simulations we performed, with results at different viscosities ($\tilde{\eta} = 1$, 2 or 3), shear moduli ($\tilde{G} = 1$, 2 or 3) and cavity sizes ($a = 4.5$ mm, in light grey, and $a = 9$ mm, in dark grey). For B, all the data collapse well and (12b) is accurate within 5% of relative error for AR<10, and 20% for $10 <$AR< 24. The collapses are not as good for A, D and β. However, the phenomenological laws are found to remain accurate within 30% for all the configurations that were simulated.

It is important to note that there is no physical grounds for Eqs. (11)-(12). They must be seen as convenient expressions for estimating the scattering function of a cylindrical cavity (defined by its equivalent radius a and aspect ratio AR) in a soft medium.

IV. REFLECTION BY AN ARRAY OF CYLINDRICAL CAVITIES

To go from the single scatterer to the array of scatterers, we modify equations (1) and (2) following the same procedure that allowed us to go from Eq. (7) to (11), *i.e.* by introducing an effective scattering radius (A), an effective resonant frequency (B), a new shear damping (β) and an effective radiative damping (D). It leads to

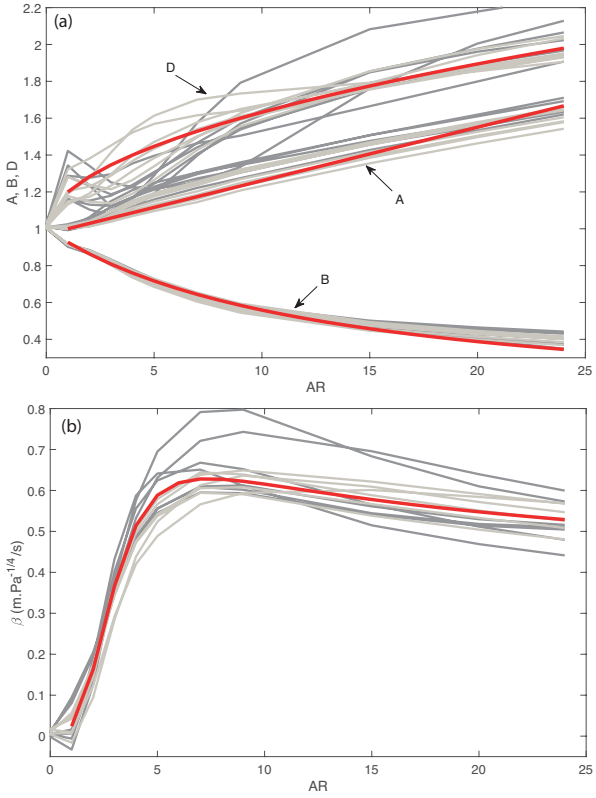

FIG. 8. Comparison between the phenomenological laws (12), in red, and the values obtained by fitting the results of the simulations, in grey. Top graph (a) shows the results for A, B and D, bottom one (b) for β. For the data from numerical simulations, two sizes of cylinder were investigated: $a = 4.5$ mm (light grey) and $a = 9$ mm (dark grey).

$$r_{\text{cyl}} = \frac{\mathrm{i}KAa}{\left(B\frac{\omega_0}{\omega}\right)^2 - J - \mathrm{i}(B^2\delta + \beta\frac{G^{1/4}}{a\omega} + DKa)}, \qquad (13)$$
$$t_{\text{cyl}} = 1 + r_{\text{cyl}}, \qquad (14)$$

with $J = 1 - KaD\sin(kd/\sqrt{\pi})$. As shown in Fig. 9, these new expressions allow us to capture the amplitudes of reflection found in Fig. 2 for metascreens with AR=1 and AR=10 on a perfect reflector. As an indicator of the role played by the geometry of the cylinders, we monitored how the minimum of reflection was changing with AR. The inset of Fig. 9 reports the frequency (f_{min}) and the value (r_{min}) of this minimum for values of AR ranging from 1 to 24. We see that our phenomenological formula predicts reasonably well the effect of AR.

Phenomenological laws (12) were established by analyzing numerical data obtained at a particular zone in the space of parameters. In other words, we cannot be sure that they will be accurate if the physical parameters are very different. For instance, for much larger cavities in a significantly more viscous

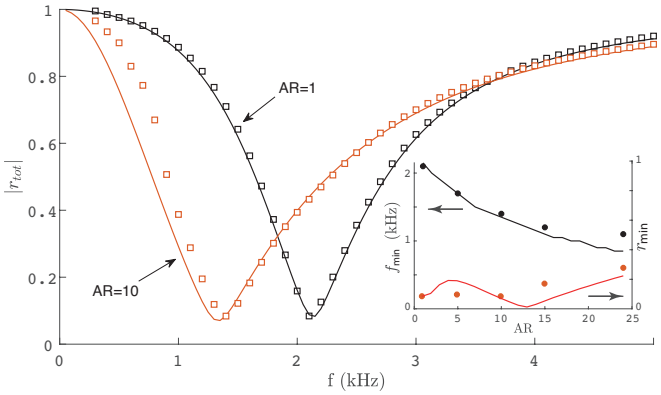

FIG. 9. Amplitude of the total reflection for metascreens with cylindrical cavities on a perfect reflector. Results of the numerical simulations (symbols, like in Fig. 2) are compared to analytical law $|(1+3r_{cyl})/(1-r_{cyl})|$, with phenomenological equation (13) for r_{cyl} (solid lines). Inset: comparison between the simulations and the phenomenological law for the frequency and amplitude of the minimum of reflection as a function of AR.

elastomer, it might be necessary to establish new phenomenological laws. However, as a test of robustness, we compared our model to experimental results available in the literature. Calvo *et al.*[14] measured the transmission through an array of cylinders with $H = 5\,\mu$m and $R = 60\,\mu$m ($AR = 24$), separated by $d = 300\,\mu$m, imbedded in a $e = 700\,\mu$m thick elastomer. Fig. 10 shows that their results (symbols) are well described by our phenomenological law (solid line). Note that multiple reflections within the slab of elastomer need to be taken into account, and that we took the rheological law given by Sharma et al.[15] for the elastomer.

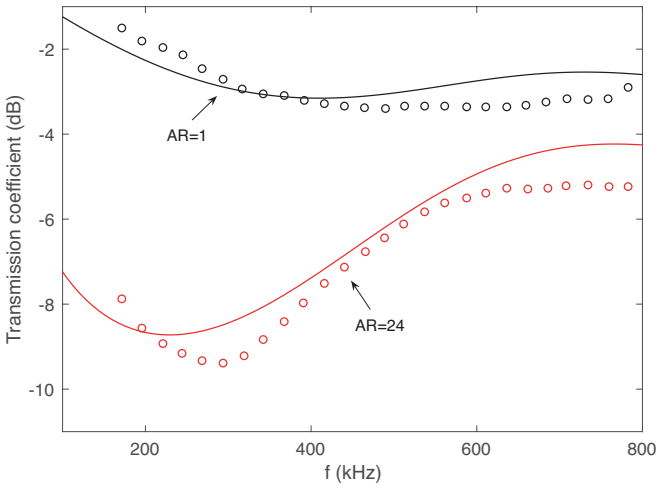

FIG. 10. Comparison between measurements (symbols) and equation (14) (lines) for the transmission through an array of cylindrical cavities with AR=1 (black) and AR=24 (red). Experimental data are reproduced from Fig. 6 in Calvo *et al.*[14]

As the phenomenological model is able to predict the influence of the cylinders aspect ratio, we can investigate how this additional parameter can be used for the design of thin absorbers. Let us come back to the case we considered in section II and see how we can minimize the reflection at 2.15 kHz with cylinders. From our numerical results on scattering by cylinders, there are two new aspects compared to the spherical case. First, cylinders resonate at a lower frequency, which means that smaller cavities can be used. Secondly, cylinders show an additional source of loss: they can emit shear waves. This can be useful because losses increase the broadness of the absorption. Let us select an aspect ratio of $AR = 10$ for example, for which shear wave losses are close to their maximum according to Fig. 8b. With such an AR, Eq. (12b) predicts a resonance frequency divided by a factor 1.8, which means that the radius of 4.5 mm for the sphere can be decreased to an equivalent radius of $a = 2.5$ mm for the $AR = 10$ cylinder. The next step is to find the optimal distance between the cavities. The criterion is sill to obtain $r = -1/3$. But the simple relationship $\delta = 2Ka$ for the spherical case now becomes $B^2\delta + \beta G^{1/4}/(a\omega) = Ka(3A - D)$, which is less straightforward. In practice, it is easier to directly plot the total reflection r_{tot} predicted by the phenomenological model for different values of a and d, and select the couple of parameters that gives the best result. We find that $a = 2.7$ mm and $d = 75$ mm lead to the total reflection plotted in red in figure 11. Numerical simulations (symbols) confirm the prediction of the model. Compared with the previous optimization for spheres (recalled in black in Fig. 11), the cylinders lead to a better performance in terms of frequency bandwidth, with a a thinner structure (see drawings in Fig. 11).

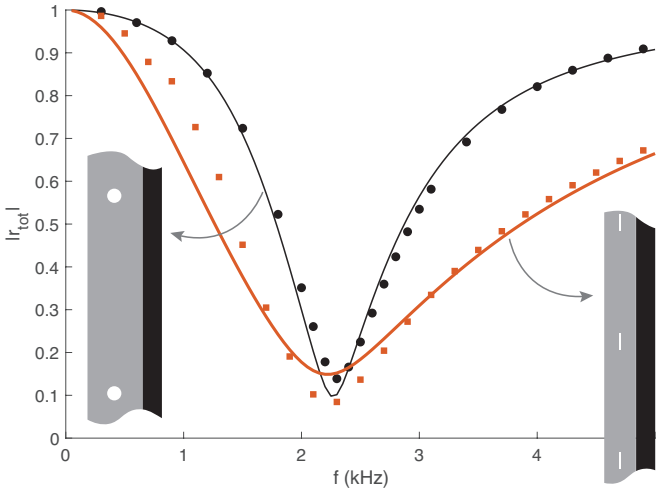

FIG. 11. Illustration of the use of the phenomenological law for optimizing a super-absorber with cylindrical cavities. The model predicts better performance with a thinner structure when the ability of cylinders to emit shear waves is exploited. In black, the results for spherical cavities (like in figure 2) with $a = 4.5$ mm, $d = 125$ mm and $e = 35$ mm. In red, for cylindrical cavities with $AR = 10$, $a = 2.7$ mm (*i.e.* $H = 1$ mm and $R = 10.2$ mm), $d = 75$ mm and $e = 20$ mm. Symbols show results of the numerical simulations, lines correspond to the prediction of the model.

V. CONCLUSION

By investigating the acoustic scattering of a longitudinal wave by a cylindrical cavity, we proposed a phenomenological extension of a model we previously developed for the transmission and reflection by an array of spherical cavities in a soft elastic solid. The effect of the shape of the cylinder, of radius R and height H, can be accounted for by two geometrical parameters: the radius of the sphere of equivalent volume $a = (3R^2H/4)^{1/3}$, and the aspect ratio AR$= 2R/H$. Flat cylinders are found to be appealing in the perspective of low frequency absorption: (1) they resonate at a lower frequency than their spherical equivalent, (2) they can convert part of the incoming longitudinal wave energy into shear wave energy. These two new characteristics can be used for the design of thinner acoustic absorbers, which are efficient on a broader frequency range. Our phenomenological model can be a convenient tool for quickly selecting the best geometry (volume, aspect ratio of the cylinders, and spacing between them) for obtaining good performance at a desired frequency. However, it should be used with caution because it has been established from a limited number of simulations, within a given range of physical parameters. Deviations may occur if one considers geometries, frequencies, or elastomer properties that are very different from the cases investigated here.

As a final note, let us remark that if flat cylinders are promising from the perspective of acoustic performance, they may be a problem for the robustness of an absorber regarding static pressure. Indeed, in underwater applications, the perforated soft panel is subject to a high static pressure, which can deform the cavities.[20–22] In this case, there is a risk that cylinders that are too flat collapse, thus losing their acoustical properties.

The data that support the findings of this study are available from the corresponding author upon reasonable request.

ACKNOWLEDGMENTS

This research was partially funded by LABEX WIFI (Laboratory of Excellence within the French Program "Investments for the Future") under references ANR-10-LABX-24 and ANR-10-IDEX-0001-02 PSL*.

[1] E. Meyer, K. Brendel, and K. Tamm, "Pulsation oscillations of cavities in rubber," The Journal of the Acoustical Society of America **30**, 1116–1124 (1958).

[2] G. Gaunaurd and H. Überall, "Theory of resonant scattering from spherical cavities in elastic and viscoelastic media," The Journal of the Acoustical Society of America **63**, 1699–1712 (1978).

[3] R. Lane, "Absorption mechanisms for waterborne sound in alberich anechoic layers," Ultrasonics **19**, 28–30 (1981).

[4] G. Gaunaurd and H. Überall, "Resonance theory of the effective properties of perforated solids," The Journal of the Acoustical Society of America **71**, 282–295 (1982).

[5] A.-C. Hladky-Hennion and J.-N. Decarpigny, "Analysis of the scattering of a plane acoustic wave by a doubly periodic structure using the finite element method: Application to alberich anechoic coatings," The Journal of the Acoustical Society of America **90**, 3356–3367 (1991).

[6] S. M. Ivansson, "Sound absorption by viscoelastic coatings with periodically distributed cavities," The Journal of the Acoustical Society of America **119**, 3558–3567 (2006).

[7] A. J. Hicks, M. R. Haberman, and P. S. Wilson, "A thin-panel underwater acoustic absorber," The Journal of the Acoustical Society of America **136**, 2098–2098 (2014).

[8] J. Zhong, H. Zhao, H. Yang, J. Yin, and J. Wen, "On the accuracy and optimization application of an axisymmetric simplified model for underwater sound absorption of anechoic coatings," Applied Acoustics **145**, 104–111 (2019).

[9] V. Leroy, A. Strybulevych, M. Scanlon, and J. Page, "Transmission of ultrasound through a single layer of bubbles," The European Physical Journal E **29**, 123–130 (2009).

[10] G. S. Sharma, A. Skvortsov, I. MacGillivray, and N. Kessissoglou, "Acoustic performance of gratings of cylindrical voids in a soft elastic medium with a steel backing," The Journal of the Acoustical Society of America **141**, 4694–4704 (2017).

[11] S. M. Ivansson, "Numerical design of alberich anechoic coatings with superellipsoidal cavities of mixed sizes," The Journal of the Acoustical Society of America **124**, 1974–1984 (2008).

[12] D. C. Calvo, A. L. Thangawng, and C. N. Layman, "Low-frequency resonance of an oblate spheroidal cavity in a soft elastic medium," The Journal of the Acoustical Society of America **132**, EL1–EL7 (2012).

[13] A. Skvortsov, I. MacGillivray, G. S. Sharma, and N. Kessissoglou, "Sound scattering by a lattice of resonant inclusions in a soft medium," Physical Review E **99**, 063006 (2019).

[14] D. C. Calvo, A. L. Thangawng, C. N. Layman Jr, R. Casalini, and S. F. Othman, "Underwater sound transmission through arrays of disk cavities in a soft elastic medium," The Journal of the Acoustical Society of America **138**, 2537–2547 (2015).

[15] G. S. Sharma, A. Skvortsov, I. MacGillivray, and N. Kessissoglou, "On superscattering of sound waves by a lattice of disk-shaped cavities in a soft material," Applied Physics Letters **116**, 041602 (2020).

[16] T. Meng, "Simplified model for predicting acoustic performance of an underwater sound absorption coating," Journal of Vibration and Control **20**, 339–354 (2014).

[17] V. Leroy, A. Strybulevych, M. Lanoy, F. Lemoult, A. Tourin, and J. H. Page, "Superabsorption of acoustic waves with bubble metascreens," Physical Review B **91**, 020301 (2015).

[18] M. Strasberg, "The pulsation frequency of nonspherical gas bubbles in liquids," The Journal of the Acoustical Society of America **25**, 536–537 (1953).

[19] K. S. Spratt, M. F. Hamilton, K. M. Lee, and P. S. Wilson, "Radiation damping of, and scattering from, an arbitrarily shaped bubble," The Journal of the Acoustical Society of America **142**, 160–166 (2017).

[20] G. Gaunaurd, E. Callen, and J. Barlow, "Pressure effects on the dynamic effective properties of resonating perforated elastomers," The Journal of the Acoustical Society of America **76**, 173–177 (1984).

[21] J.-B. Dupont, P. Lamy, and Y. Renou, "Transparence acoustique de revetement type alberich sous forte pression d'eau : methode de simulation couplée (in french)," 24eme Congrès Francais de Mécanique (2019).

[22] M. Thieury, A. Tourin, J. Dassé, and V. Leroy, "Effect of hydrostatic pressure on a bubble anechoic metascreen," 13th Internaional Congress on Artificial Materials for Novel Wave Phenomena - Metamaterials (2019).